A Two-Stage Data-Driven Multi-Energy Management Considering Demand Response

Pengfei Zhao
Department of Electronic and
Electrical Engineering
University of Bath
Bath, United Kingdom
P.zhao@bath.ac.uk

Chenghong Gu[†]
Department of Electronic and
Electrical Engineering
University of Bath
Bath, United Kingdom
C.Gu@bath.ac.uk

Zhidong Cao
The State Key Laboratory of
Management and Control for
Complex Systems,
Institute of Automation, Chinese
Academy of Sciences,
Beijing, China
Zhidong.Cao@ia.ac.cn

Yue Xiang
College of Electrical Engineering
Sichuan University
Chengdu, China
xiang@scu.edu.cn

Xiaohe Yan
State Key Lab of Internet of Things
for Smart City
Macau University
Macau, China
xiaohe_yan@yahoo.com

Da Huo
School of Engineering,
Newcastle University
Newcastle, United Kingdom
Da.Huo@newcastle.ac.uk

ABSTRACT

This paper proposes an innovative two-stage data-driven optimization framework for a multi-energy system. Enormous energy conversion technologies are incorporated in the system to enhance the overall energy utilization efficiency, i.e., combined heat and power, power-to-gas, gas furnace, and ground source heat pump. Furthermore, a demand response program is adopted for stimulating the load shift of customers. Accordingly, both the economic performance and system reliability can be improved. The endogenous solar generation brings about high uncertainty and variability, which affects the decision making of the system operator. Therefore, a two-stage data-driven distributionally robust optimization (TSDRO) method is utilized to capture the uncertainty. A tractable semidefinite programming reformulation is obtained based on the duality theory. Case studies are implemented to demonstrate the effectiveness of applying the TSDRO on energy management.

CCS CONCEPTS

• Power system operation • Optimization method

KEYWORDS

Demand response, Energy hub systems, Multi-energy systems.

1 NOMENCLATURE

This section presents the description of the sets, parameters and variables, which are used in the mathematical modelling.

A. Sets

T	Set of time periods.

B. Parameters

η_{P2G}	Conversion efficiency of power-to-gas (P2G) facility.
HHV	Higher heat value of combined heat and power (CHP).
η_e, η_{th}	Electrical and thermal efficiency of CHP.
η_{P2G}	Electrical efficiency of electrolyser.
η_f, η_{re}	Efficiency of GF and solar power generation.
COP	Coefficient of performance.
$\overline{P_{g,CHP}}, \overline{P_{e,HP}}, \overline{P_{g,GF}}$	Maximum input limit of CHP, ground source heat pump (GSHP) and gas furnace (GF).
$\underline{P_{g,CHP}}, \underline{P_{e,HP}}, \underline{P_{g,GF}}$	Minimum input limit of CHP, GSHP and GF.
$\overline{P_{hs}^{ch}}, \underline{P_{hs}^{ch}}$	Maximum and minimum limit of charging power of heat storage.
$\overline{P_{hs}^{dch}}, \underline{P_{hs}^{dch}}$	Maximum and minimum limit of discharging power of heat storage.
$P_{hs}^{stb}(t)$	Standby power loss of heat storage at time t.
$E_{hs,min}, E_{hs,max}$	Minimum and maximum energy for heat storage.
$\eta_{hs}^{ch}, \eta_{hs}^{dch}$	Charging and discharging efficiency of heat storage.
$\overline{P_b^{ch}}, \underline{P_b^{ch}}$	Maximum and minimum limit of charging power of battery.
$\overline{P_b^{dch}}, \underline{P_b^{dch}}$	Maximum and minimum limit of discharging power of battery.
$E_{b,min}, E_{b,max}$	Minimum and maximum energy for battery.
$\eta_b^{ch}, \eta_b^{dch}$	Charging and discharging efficiency of battery.
$\omega_f(t)$	Solar generation forecast at time t.
$\overline{P_{ele}}, \underline{P_{ele}}$	Maximum and minimum limit of electricity purchase.
$\overline{P_{gas}}, \underline{P_{gas}}$	Maximum and minimum limit of gas purchase.
$\pi_{ele}(t), \pi_{gas}(t)$	Electricity and gas purchase cost at time t.
$L_e(t), L_{th}(t)$	Electricity and heating demand at time t.
$DR_{ele,max}, DR_{th,max}$	Maximum limit for demand response coefficient.

C. Variables

EC_{ele}, EC_{gas}	Energy purchase cost of power and gas.
$\omega_{P2G}(t), P_{g,P2G}(t)$	Input and output of P2G electrolyzer.
$P_{g,CHP}(t), P_{e,HP}(t), P_{g,GF}(t)$	Input of CHP, GSHP and GF.
$P_{CHP,Eout}(t), P_{CHP,Hout}(t), P_{HP,out}(t), P_{GF,out}(t)$	Output of CHP, HP and GF.
$P_{hs}^{ch}(t), P_{hs}^{dch}(t)$	Charging and discharging power of heat storage at time t.
$u_{hs}^{ch}(t), u_{hs}^{dch}(t)$	Charging and discharging status of heat storage at time t.
$P_b^{ch}(t), P_b^{dch}(t)$	Charging and discharging power of battery at time t.
$u_b^{ch}(t), u_b^{dch}(t)$	Charging and discharging status of battery at time t.
$E_{hs}(t), E_b(t)$	Remaining capacity of heat and battery storage.
$\omega_r(t)$	Scheduled solar power generation at time t.
$P_{ele}(t)$	Electricity purchase at time t.
$P_{gas}(t)$	Gas purchase at time t.
$v_e(t), v_g(t)$	Dispatch factors of electricity and gas.
$P_{ele}^{DR}(t), L_{ele}^{DR}(t)$	Shifted and resulting electricity load under demand response at time t.
$P_{th}^{DR}(t), L_{th}^{DR}(t)$	Shifted and resulting heating load under demand response at time t.

2 INTRODUCTION

The modern energy systems tend to strengthen the linkage among multi-energy systems (MESs), which significantly aggregates the local generation, distribution and consumption level by end energy customers with new technologies [1, 2]. This trend requires a basic understanding of the modelling, operation and conversion among all the sub-energy systems. Emerging research efforts are dedicated to resolving the challenges of decarbonization, facilitating renewable penetration and reducing the operation cost based on MESs [3-5].

However, interdependencies and strong couplings have been always the main challenges without an effective solution [6]. Moreover, another limitation of the current research is that the inherent uncertainties cannot be well handled due to the limited data availability, which inevitably affects the system economic performance. Energy hub is a smart local energy management system from the multi-energy perspective, which relies on enormous conversions among multi-energy vectors [7, 8]. The energy hub is an interface between local energy producers and consumers with coordination and complementation of multi-energy vectors to economically and effectively satisfy loads. To sum up, there are two challenges with respect to multi-energy management: i) the enormous interdependencies and strong couplings among multi-energy vectors are required to be effectively modelled to enhance the overall energy efficiency; and ii) the renewable uncertainty needs an effective optimization framework with mild conservatism and sufficient data availability.

This paper aims to provide an optimal multi-energy management scheme for MESs. The uncertain renewable variation and fluctuation are handled by a hierarchical two-stage data-driven approach, which enables to determine an initial day-ahead operation scheme based on renewable forecast and take adaptive recourse actions with renewable realization. Cross-vector demand response (DR) is employed to alter the energy users' consumption pattern and thus to reduce the operation cost. To address challenges of modelling energy interdependencies and improper uncertainty treatment, this paper proposes a two-stage data-driven energy hub scheduling considering DR programs, which aims to minimize the daily operation cost. The energy hub is equipped with photovoltaic (PV), energy converters and energy storage systems. The cross-vector DR includes the participation from customers on electricity and heat loads, which helps to reduce the daily operation cost of the energy hub and shift the peak-load. Multiple energy interdependencies and strong energy couplings are considered, including power-to-gas, power-to-heat and heat-to-power. The PV uncertainty is captured via a two-stage DRO framework. Moment information is utilized to construct the ambiguity set. The main advantages of this paper are as follows:

- This paper designs a comprehensive model of the multi-vector system in the form of an energy hub, where the extensive energy conversion is modelled. The proposed model is effective for improving the mutlti-energy utilization efficiency based on conversion technologies.
- Both DR program for heat and electric load are considered to provide additional flexibility for energy hub operators and the grid.
- A two-stage data-driven DRO model is utilized for hedging against PV uncertainty in terms of limited data set and mild robustness. A moment-based ambiguity set is modelled to capture the PV uncertainty. Dual reformulations are made and a semidefinite programming is finally obtained with ensured tractability.

3   RELATED WORK

Paper [9] proposes an optimal energy flow model for interconnected energy hubs considering network constraints. The intermittency of renewable generation is handled by a stochastic optimization (SO) based chance-constrained programming. A Cornish-Fisher expansion is utilized to solve the reformulated problem. A distributionally robust optimization (DRO) is applied for energy hub operation considering the multimodality of PV generation [10]. In order to ensure both the voltage security and economic performance, paper [11] designs a volt-var optimization in MES. A reinforcement learning-based data-driven optimization is designed for optimal operation of MESs [12]. The scheduling decisions of electric vehicles and residential appliances are subsequently obtained.

DR is a viable solution for network operators to stimulate energy customers to shift the flexible load profile. Customers are willing to alter their energy consumption patterns in response to
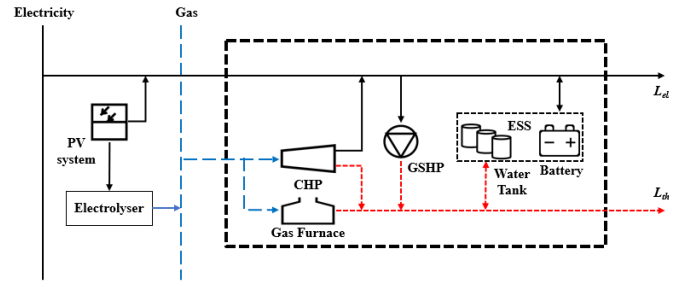

Fig. 1. Overview schematic of the energy hub.

energy price signals. DR in EHS has been investigated in many existing papers. Paper [13] proposes an integrated model for optimal planning of EHS considering DR and renewable energy. A two-stage SO is applied to assess the impacts of uncertainties. The effective DR is embedded into the operational sub-problem. Instead of conventional DR, an integrated DR is proposed in [14] for multiple energy carriers. The interactions between EHSs are modelled as an ordinal potential game. EHSs can participate in DR via switching energy sources during peak demand hours. Paper [15] proposes an optimal probabilistic operation model of EHS with DR. The multi-vector DR contributes to diminishing the operation cost of EHS with customer participation.

To capture the inherent uncertainties in power system operations such as uncertain renewable generation, load demand and contingency events, robust optimization (RO) has been extensively applied. RO makes decisions based on the worst-case scenario, which effectively improves the optimization reliability. Paper [16] proposes a dispatch model of a large-scale hybrid wind/PV/hydro/thermal power system with RO framework. The intermittent power supply is modelled based on the flexible control of robustness. An optimal bidding strategy in a day-ahead microgrid market is proposed in [17]. The intermittency of distributed generation, load variation, and real-time market prices are handled by RO. Paper [18] designs a two-stage RO framework for distribution system reconfiguration, considering load uncertainty. The first stage is to configure the network and the second stage determines the optimal AC power flow. Another classic optimization to capture uncertainties is SO. Compared with RO, SO is another extreme as it assumes the explicit uncertainty distributions [19-21]. Notwithstanding, the solutions are more accurate based on a large number of sample sets and it causes low computational efficiency. Moreover, it is always challenging to obtain sufficient historical data to model real distributions. On the contrary, RO avoids the over-optimistic assumption of uncertainty distributions and provides reliable and computational-efficient solutions.

For DRO, the ambiguity set is constructed by statistical information, such as moment, to restricting possible distributions. Based on more valuable distribution information, research finds that the best estimate of the distribution can be obtained through the statistical fitting. Accordingly, statistical distance information can be added in the ambiguity set and thus the size of the ambiguity set can be controlled. In addition, compared with RO,

DRO determines expected results over all possible distributions, which are less-conservative. Paper [22] proposes a DRO-based multi-period economic dispatch based on a segeragated linear decision rule. Case studies have demonstrated the effectiveness over the traditional single-period DRO framework. A distributionally robust operation of an electric vehicle aggregator is given in [23], which is proved to outperform RO and SO.

4 ENERGY HUB SYSTEM MODELLING

The mathematical modelling of energy hub is presented in this section, including solar PV panels, heat pump (HP), gas furnace (GF), power-to-gas (P2G), combined heat and power (CHP) and a hybrid energy storage system (ESS).

Fig. 1 depicts the proposed energy hub structure, where the power, gas and heat flow are represented by black, blue and red lines. CHP consumes gas and generates power and heat simultaneously. GF converts gas to heat. GSHP enables to convert power to heat with 300% efficiency. The ESS stores both power and heat based on the surplus energy [24]. The PV system generates solar power via PV panels. However, the generation contains fluctuation due to the unpredicted clouding and weather conditions, which causes PV uncertainty.

4.1 Objective function

The energy generation, storage, consumption and extensive energy conversions are realized in proposed energy hub among power, gas and heat. The power and gas purchase from the external markets are the original energy source. The P2G electrolyser converts power to gas with an efficiency of 80%. The ESS is used to store the surplus energy for later usage. This paper adopts a two-stage optimization framework for energy hub scheduling including the day-ahead initial operation scheme based on PV forecast and the real-time adjustive redispatch based on the more accurate PV generation. The objective function shown in (1) to minimize the energy purchase cost. The first-stage objective minimizes the day-ahead operation cost based on PV forecast. And the second-stage objective is to minimize the penalty cost caused by energy purchase deviation (EC'_{ele} and EC'_{gas}).

$$Obj_1 = \min \sum_{t \in T} EC_{ele} + EC_{gas}, \forall t \in T \quad (1)$$
$$Obj_2 = \min \sum_{t \in T} EC'_{ele} + EC'_{gas}, \forall t \in T$$
s.t. (2)-(25)

4.2 Technical Constraint Formulation

4.2.1 Conversion Constraints

The converted output of P2G, CHP, HP, GF are given in (2)-(6), respectively. Constraints (7)-(9) limit the input of CHP, HP and GF.

$$P_{g,P2G}(t) = \eta_e \frac{\omega_{P2G}(t)}{HHV} , \forall t \in T \quad (2)$$

$$P_{CHP,Eout}(t) = \eta_e P_{g,CHP}(t) , \forall t \in T \quad (3)$$
$$P_{CHP,Hout}(t) = \eta_{th} P_{g,CHP}(t) , \forall t \in T \quad (4)$$
$$P_{HP,out}(t) = COP\ P_{e,HP}(t) , \forall t \in T \quad (5)$$
$$P_{GF,out}(t) = \eta_f P_{g,GF}(t) , \forall t \in T \quad (6)$$
$$\underline{P_{g,CHP}} \le P_{g,CHP}(t) \le \overline{P_{g,CHP}} , \forall t \in T \quad (7)$$
$$\underline{P_{e,HP}} \le P_{e,HP}(t) \le \overline{P_{e,HP}} , \forall t \in T \quad (8)$$
$$\underline{P_{g,GF}} \le P_{g,GF}(t) \le \overline{P_{g,GF}} , \forall t \in T \quad (9)$$

4.2.2 ESS Constraints

This paper designs a power-heat hybrid ESS including battery storage and heat storage. The modelling of ESS is given in (10)-(14), where $\{\cdot\}$ represents $\{hs, b\}$. Constraints (10) and (11) limit the charging and discharging power and heat. The binary variables $u^{ch}_{\{\cdot\}}(t)$ and $u^{dch}_{\{\cdot\}}(t)$ are used to ensure the charging and discharging behaviour are not happening in the same time. Constraints (13) and (14) regulate the remaining energy of ESS.

$$u^{ch}_{\{\cdot\}}(t)\underline{P^{ch}_{\{\cdot\}}} \le P^{ch}_{\{\cdot\}}(t) \le u^{ch}_{\{\cdot\}}(t)\overline{P^{ch}_{\{\cdot\}}} , \forall t \in T \quad (10)$$

$$u^{dch}_{\{\cdot\}}(t)\underline{P^{dch}_{\{\cdot\}}} \le P^{dch}_{\{\cdot\}}(t) \le u^{dch}_{\{\cdot\}}(t)\overline{P^{dch}_{\{\cdot\}}} , \forall t \in T \quad (11)$$

$$u^{ch}_{\{\cdot\}}(t) + u^{dch}_{\{\cdot\}}(t) \le 1, \forall t \in T \quad (12)$$

$$E_{\{\cdot\}}(t) = E_{\{\cdot\}}(t-1) + \sum_1^t P^{ch}_{\{\cdot\}}(t)\eta^{ch}_{\{\cdot\}} - P^{dch}_{\{\cdot\}}(t)/ \quad (13)$$
$$\eta^{dch}_{\{\cdot\}} + P^{stb}_{\{\cdot\}}(t), \ \forall t \in 2...T$$

$$E_{\{\cdot\},min} \le E_{\{\cdot\}}(t) \le E_{\{\cdot\},max}, \forall t \in T \quad (14)$$

4.2.3 Constraints of Energy Purchase

The power and gas purchase from the external market supplies the energy hub with the modelling given in (15) and (16). Noted that $\{\cdot\}$ denotes $\{ele, gas\}$.

$$\underline{P_{\{\cdot\}}} \le P_{\{\cdot\}}(t) \le \overline{P_{\{\cdot\}}} \quad (15)$$

$$EC_{\{\cdot\}} = \pi_{\{\cdot\}}(t)\ P_{\{\cdot\}}(t), \forall t \in T \quad (16)$$

4.2.4 Energy Balance Conditions

The balancing condition (coupling matrix) of the energy hub modelling is shown in (17) to guarantee the overall balance between the input and output.

$$\begin{bmatrix} L_{ele}(t) + P_b(t) \\ L_{th}(t) + P_{hs}(t) \end{bmatrix} =$$
$$\begin{bmatrix} 1 - v_e(t) & \eta_{re}(1 - v_e(t)) & v_g(t)\eta_e(1 - v_e(t)) \\ v_e(t)COP & v_e(t)\eta_{re}COP & v_g(t)(\eta_{th} + \eta_e v_e(t)COP + \eta_f - v_g(t)\eta_f) \end{bmatrix}$$
$$\times \begin{bmatrix} P_{ele}(t) \\ \omega_r(t) - \omega_{P2G}(t) \\ P_{gas}(t) + P_{g,P2G}(t) \end{bmatrix} \quad (17)$$

4.2.5 Demand Response Conditions

Energy hub operator implements DR program to encourage the participation of energy customers for gaining economic benefit, i.e., lower energy price at certain time periods is applied which

stimulates customers to alter their energy consumption profile. The shifted load demand for power and heat are given in (18) and (22) under the maximum limits in (19) and (23). Constraints (20) and (24) regulate the demand deviation owing to the DR program. Equations (21) and (25) guarantees that the overall demand is unchanged.

$$L_{ele}^{DR}(t) = L_{ele}(t) + P_{ele}^{DR}(t) \, , \forall t \in T \qquad (18)$$

$$L_{ele}^{DR}(t) \leq L_{ele}^{DR,max} \qquad (19)$$

$$\left| P_{ele}^{DR}(t) \right| \leq L_{ele}(t) DR_{ele,max} \, , \forall t \in T \qquad (20)$$

$$\sum_{t=1}^{T} P_{ele}^{DR}(t) = 0 \, , \forall t \in T \qquad (21)$$

$$L_{th}^{DR}(t) = L_{th}(t) + P_{th}^{DR}(t) \, , \forall t \in T \qquad (22)$$

$$L_{th}^{DR}(t) \leq L_{th}^{DR,max} \qquad (23)$$

$$|P_{th}^{DR}(t)| \leq L_{th}(t) DR_{th,max} \, , \forall t \in T \qquad (24)$$

$$\qquad (25)$$

$$\sum_{t=1}^{T} P_{th}^{DR}(t) = 0 \, , \forall t \in T$$

Fig. 2. Flowchart of C&CG.

5 METHODOLOGY

This section proposes the method for solving the two-stage energy hub operation via DRO model. The abstract formulation and ambiguity set is given firstly, followed by the dual reformulations to ensure the computational tractability. Finally, a semidefinite programming model is obtained.

5.1 Ambiguity set modelling

The abstract formulation of the proposed model is given in (26)-(29), where the overall and second-stage objective functions are given in (26) and (28), respectively. Equation (26) is the overall ojective incorporating Obj_1 and Obj_2 in (1). And (28) explicitly describes the expected Obj_2. Equations (27) and (29) represent the constraints in the first and second stages.

$$\min_{x \in X} c'x + \sup_{Pf \in D} E_P[Q(x,\xi)] \qquad (26)$$

$$\text{s.t. } Ax \leq b, \qquad (27)$$

$$Q(x,\xi) = \min_y f'y \qquad (28)$$

$$\text{s.t. } Ex + Fy + G\xi \leq h, \qquad (29)$$

The data-driven ambiguity set is used to accommodate the statistical information of the uncertain variables. In this paper, the moment information is adopted which reflects the partial distributional information of the PV uncertainty. The fixed mean vector and covariance matrix enable to model a set of possible distributions which share the same moment information. The moment-based data-driven ambiguity set is given in (30).

$$D = \left\{ f(\xi) \middle| \begin{array}{c} P\{\xi\} = 1 \\ E\{\xi\} = \mu \\ E\{\xi\,(\xi)'\} = \Sigma + \mu\,(\mu)' \end{array} \right\} \qquad (30)$$

5.2 Dual reformulations

This section proposes two dual reformulations. The first dual reformulation is to merge the two sub-objectives in the first and second stages with '*sup*' eliminated. And the second dual reformulation is to transform the infinite variable cardinality to finite cardinality.

The explicit form of $\sup_{Pf \in D} E_P[Q(x,\xi)]$ can be rewritten as (31)-(35).

$$S(x)^{primal} = \max_{Pf \in D_\xi} \int_\Xi Q(x,\xi)\, Pf(\xi) d\xi \qquad (31)$$

$$\text{s.t. } Pf(\xi) \geq 0, \forall \xi \in \Xi \qquad (32)$$

$$\int_\Xi Pf(\xi) d\xi = 1 \qquad (33)$$

$$\int_\Xi \xi^m Pf(\xi) d\xi = \mu_m, \text{m=1,2, ...,} \Xi \qquad (34)$$

$$\int_\Xi \xi^m \xi^n Pf(\xi) d\xi = \Sigma_{mn} + \mu_m \mu_n, \text{m, n=1,2, ...,} \Xi \qquad (35)$$

$Pf(\xi)$ is the decision variable of (31) which is with infinite cardinality. The dual reformulation enables to transform the infinite-dimensional primal form to the dual form with tractability ensured [25]. The dual reformulation is given in (36) and (38) with dual variables ψ_0, ψ_j and Ψ_{jk}.

$$S(x)^{dual} = \min_{\Psi,\psi,\psi_0} \langle \Psi'\Theta \rangle + \psi'\mu + \psi_0 \qquad (36)$$

$$\text{s.t. } (\xi)'\Psi\xi + \psi'\xi + \psi_0 \geq Q(x,\xi), \forall \xi \in \Xi \qquad (37)$$
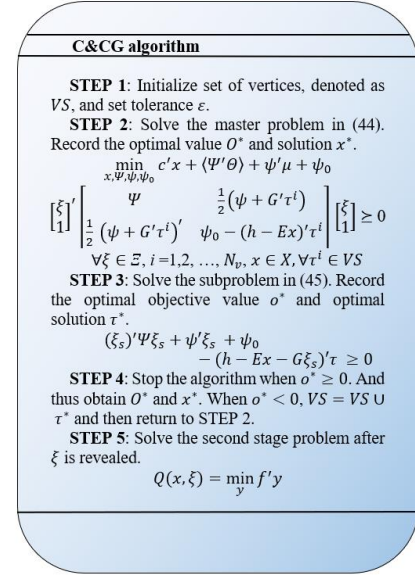
$$\min_{x \in X} c'x + S(x)^{dual} \qquad (38)$$

5.3 Semidefinite programming

Another dual reformulation is required to transform to a closed-form of $Q(x,\xi)$ [26], which is shown in (39) and (40).

$$\max_{u \in VS} \tau'(h - Ex - G\xi) \tag{39}$$

$$VS = \{\tau | F'\tau = f, \tau \leq 0\} \tag{40}$$

Equation (41) is the optimal solution of (27) and equations (42) and (43) can be obtained when (41) is substituted by (37).

$$\exists \tau \in VS: Q(x,\xi) = (h - Ex - G\xi)'\tau \tag{41}$$

$$(\xi)'\Psi\xi + \psi'\xi + \psi_0 \geq (h - Ex - G\xi)'\tau \tag{42}$$

$$\forall \xi \in \Xi, i = 1,2, \dots, N_v$$

$$(\xi)'\Psi\xi + (\psi + G'\tau^i)'\xi + \psi_0 - (h - Ex)\tau^i \geq 0 \tag{43}$$

$$\forall \xi \in \Xi, i = 1,2, \dots, N_v$$

Thus, equation (44) is the final reformulated objective function to be solved with positive quadractic function in matrix form.

$$\min_{x,\Psi,\psi,\psi_0} c'x + \langle \Psi'\Theta \rangle + \psi'\mu + \psi_0$$

$$\begin{bmatrix} \xi \\ 1 \end{bmatrix}' \begin{bmatrix} \Psi & \frac{1}{2}(\psi + G'\tau^i) \\ \frac{1}{2}(\psi + G'\tau^i)' & \psi_0 - (h - Ex)'\tau^i \end{bmatrix} \begin{bmatrix} \xi \\ 1 \end{bmatrix} \geq 0 \tag{44}$$

$$\forall \xi \in \Xi, i = 1,2, \dots, N_v, x \in X, \forall \tau^i \in VS$$

However, the remaining issues is that the vast cardinality of the extreme point set VS causes high computational burden. The proposed column and constraint generation alforithm can solve the large-scale linear models [27], which is given in Fig. 2. And equation (45) presents the sub-problem. The initial set for all the vertices is set in the first step. Then the master and sub problems are solved in turn. At each iteration, the optimal objective value is checked if it is above 0. If it is not, the set of vertices is updated to incorporate more vertices. When the terminal condition is satisfied, record the optimal value and optimal solution. Then the second-stage problem can be solved based on an expected manner.

$$(\xi_s)'\Psi\xi_s + \psi'\xi_s + \psi_0 - (h - Ex - G\xi_s)'\tau \geq 0 \tag{45}$$

6 CASE STUDIES

Case studies are conducted to show the effectiveness of the proposed two-stage data-driven energy hub management with DR. The load shift result based on DR program is given firstly. Then the economic performance and load rescheduling with different pricing schemes are given. The pricing information of real-time pricing (RTP), time-of-use (TOU) and critical peak pricing (CPP) are shown in Fig. 3 and the gas price is fixed at \$0.03/kWh [8-10]. The other technical parameters of the energy hub can be found from the previous literature of the authors [9, 10].

6.1 Impact of Demand Response

This section proposes the impact of DR programs on system operation. In Figs. 4 and 5, the altered energy patterns are given
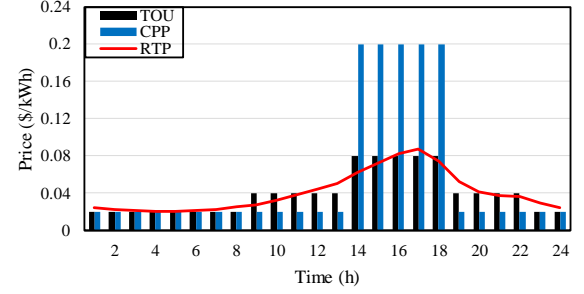

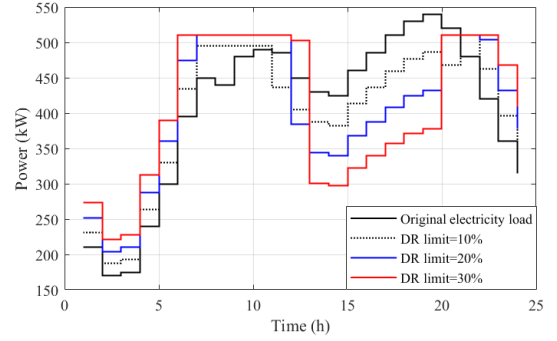Fig. 3. Pricing mechanisms of TOU, CPP and RTP.

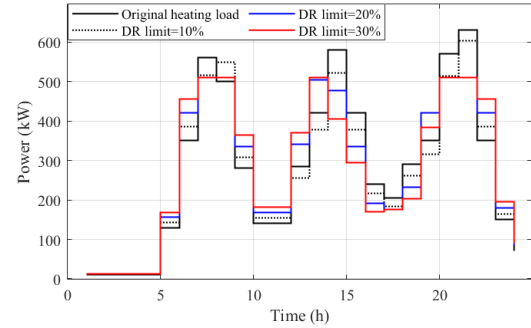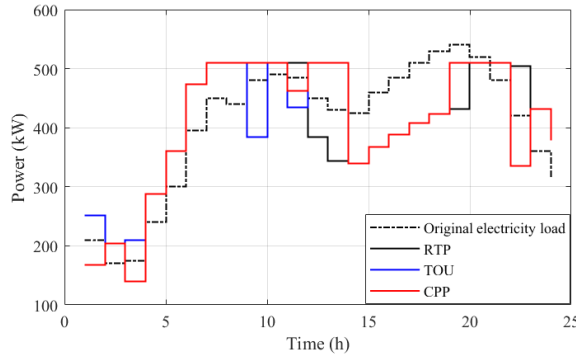Fig. 4. Electricity load under different DR programs.

Fig. 5. Heating load under different DR programs.

under different DR programs based on RTP. Fig. 6 shows that the large portion of electricity demand is added during the low-price periods, i.e., from 1:00 to 11:00. While a large amount of electricity load is reduced at the high-price periods, i.e., 13:00 to 20:00. When the DR limit ($DR_{ele,max}$) is increasing, the resulting electricity load consumption pattern is gradually deviating from the original load consumption pattern. For instance, at 19:00, the original electricity load is 540kW while it is 486kW, 432kW and 378kW under the DR limit of 10%, 20% and 30%, respectively. Similarly, Fig. 5 depicts the heating load profile under different DR limits. With the increase of DR limit, more heating load is shifted from the original heating load periods (6:00-10:00, 13:00-16:00, 20:00-22:00) to the other time periods.

Table 1: Economic Performance under Different Pricing Schemes

Economic result	RTP	TOU	CPP
Electricity purchase cost ($)	220.80	193.50	208.24
Gas purchase cost ($)	134.92	142.74	48.82
Total operation cost ($)	355.72	336.24	257.06

Fig. 6. Electricity load under different DR programs.

6.2   Application of Different Pricing Mechanisms

In this section, the comparison is made conducting three different pricing mechanisms, i.e., RTP, TOU and CPP. The economic performance of implementing the three pricing mechanisms is given in TABLE I. Noted that the hybrid uncertainty set is applied. RTP yields the highest electricity purchase cost and total operation cost. The gas purchase cost under TOU scheme is the highest but the total operation cost is $19 lower than that under RTP. The reason of the cost difference between RTP and TOU is that the proposed TOU is the approximation of RTP, which is generally lower than RTP. The lower unit purchase cost determines the lower energy purchase cost. In comparison, CPP has a totally different pricing curve than RTP and TOU, i.e., the electricity price during the peak load periods is much higher than those under RTP and TOU. The total operation cost applying CPP is only $257.06, which is 72% and 76% of the operation cost under RTP and TOU. In addition, the gas purchase cost ($48.82) is much lower than those of RTP and TOU. It is because under DR with RTP, load is extensively shifted to low-price periods. Instead of employing CHP and GF with gas consumption, the shifted electricity profile is more scheduled. In Fig. 6 the altered energy patterns are given under different DR programs among RTP, TOU and CPP. Compared with the original electricity load profile without DR participation, when applying CPP, the consumption profile changes significantly. The load from 14:00 to 18:00 is mainly shifted to 6:00-14:00 due to the extremely high electricity tariff at the peak hours.

Table 2: Economic Performance

Economic result ($)	RO	LDR-based DRO	The proposed model
First-stage cost	444	389	377
Expected Second-stage cost	0	26	21
Total cost	444	415	398

6.3   Comparison Analysis

In order to test the mathematical performance of the proposed two-stage DRO model, a single-stage RO and a DRO model based on linear decision rule are adopted for algorithm comparison. TABLE II shows the economic result of the two stages. A box uncertainty set is utilized for the single-stage RO. Both the first-stage cost and total cost are $444 without considering the second-stage recourse actions. The proposed moment-based DRO is also compared with a linear decision rule (LDR) based DRO approach, which assumes an affine relationship between the second-stage decisions and uncertain variables [22]. This method conservatively approximates the feasible region of the decision problem, which is computationally efficient. However, the less-conservatism is sacrificed. TABLE II shows that the operation cost of the two stages are $389 and $26 via LDR-based DRO. In comparison, the proposed two-stage moment-based DRO reduces the total operation cost by $17. To sum up, the proposed model mitigates the over-conservatism by RO and LDR-based DRO.

7   CONCLUSION

This paper develops a novel two-stage data-driven optimal operation of energy hub considering cross-vector DR program. The energy hub incorporates multiple energy converters, renewable energy sources and ESS. The uncertain PV generation is effectively modelled via the data-driven ambiguity set with limited distributional information to resolve the limited data availability of using SO. Case studies are conducted to demonstrate the effectiveness of the DR program. This work can benefit both the energy hub operator and customers in terms of saving the operation cost and reducing peak loads.

REFERENCES

[1]   X. Xu, J. Li, Y. Xu, Z. Xu, and C. S. Lai, "A Two-stage Game-theoretic Method for Residential PV Panels Planning Considering Energy Sharing Mechanism," *IEEE Transactions on Power Systems,* pp. 1-1, 2020, doi: 10.1109/TPWRS.2020.2985765.
[2]   C. Gu, C. Tang, Y. Xiang, and D. Xie, "Power-to-gas management using robust optimisation in integrated energy systems," *Applied Energy,* vol. 236, pp. 681-689, 2019/02/15/ 2019, doi: https://doi.org/10.1016/j.apenergy.2018.12.028.
[3]   S. Li, H. He, and J. Li, "Big data driven lithium-ion battery modeling method based on SDAE-ELM algorithm and data pre-processing technology," *Applied Energy,* vol. 242, pp.

1259-1273, 2019/05/15/ 2019, doi: https://doi.org/10.1016/j.apenergy.2019.03.154.

[4] S. Li, J. Li, C. Su, and Q. Yang, "Optimization of Bi-Directional V2G Behavior With Active Battery Anti-Aging Scheduling," *IEEE Access,* vol. 8, pp. 11186-11196, 2020, doi: 10.1109/ACCESS.2020.2964699.

[5] P. Zhao, C. Gu, Z. Hu, X. I. E. D, I. Hernando-Gil, and Y. Shen, "Distributionally Robust Hydrogen Optimization with Ensured Security and Multi-Energy Couplings," *IEEE Transactions on Power Systems,* pp. 1-1, 2020, doi: 10.1109/TPWRS.2020.3005991.

[6] Y. Shen, C. Gu, Z. Ma, X. Yang, and P. Zhao, "A Two-Stage Resilience Enhancement for Distribution Systems Under Hurricane Attacks," *IEEE Systems Journal,* pp. 1-9, 2020, doi: 10.1109/JSYST.2020.2997186.

[7] P. Zhao, C. Gu, and D. Huo, "Two-Stage Coordinated Risk Mitigation Strategy for Integrated Electricity and Gas Systems under Malicious False Data Injections," *IEEE Transactions on Power Systems,* pp. 1-1, 2020, doi: 10.1109/TPWRS.2020.2986455.

[8] P. Zhao, H. Wu, C. Gu, and I. Hernando-Gil, "Optimal home energy management under hybrid photovoltaic-storage uncertainty: a distributionally robust chance-constrained approach," *IET Renewable Power Generation,* vol. 13, no. 11, pp. 1911-1919, 2019, doi: 10.1049/iet-rpg.2018.6169.

[9] D. Huo, C. Gu, K. Ma, W. Wei, Y. Xiang, and S. L. Blond, "Chance-Constrained Optimization for Multienergy Hub Systems in a Smart City," *IEEE Transactions on Industrial Electronics,* vol. 66, no. 2, pp. 1402-1412, 2019, doi: 10.1109/TIE.2018.2863197.

[10] P. Zhao, C. Gu, D. Huo, Y. Shen, and I. Hernando-Gil, "Two-Stage Distributionally Robust Optimization for Energy Hub Systems," *IEEE Transactions on Industrial Informatics,* vol. 16, no. 5, pp. 3460-3469, 2020, doi: 10.1109/TII.2019.2938444.

[11] P. Zhao, C. Gu, Y. Xiang, X. Zhang, Y. Shen, and S. Li, "Reactive Power Optimization in Integrated Electricity and Gas Systems," *IEEE Systems Journal,* pp. 1-11, 2020, doi: 10.1109/JSYST.2020.2992583.

[12] X. Xu, Y. Jia, Y. Xu, Z. Xu, S. Chai, and C. S. Lai, "A Multi-agent Reinforcement Learning based Data-driven Method for Home Energy Management," *IEEE Transactions on Smart Grid,* pp. 1-1, 2020, doi: 10.1109/TSG.2020.2971427.

[13] S. A. Mansouri, A. Ahmarinejad, M. Ansarian, M. S. Javadi, and J. P. S. Catalao, "Stochastic planning and operation of energy hubs considering demand response programs using Benders decomposition approach," *International Journal of Electrical Power & Energy Systems,* vol. 120, p. 106030, 2020/09/01/ 2020, doi: https://doi.org/10.1016/j.ijepes.2020.106030.

[14] S. Bahrami and A. Sheikhi, "From Demand Response in Smart Grid Toward Integrated Demand Response in Smart Energy Hub," *IEEE Transactions on Smart Grid,* vol. 7, no. 2, pp. 650-658, 2016, doi: 10.1109/TSG.2015.2464374.

[15] M. Alipour, K. Zare, and M. Abapour, "MINLP Probabilistic Scheduling Model for Demand Response Programs Integrated Energy Hubs," *IEEE Transactions on Industrial Informatics,* vol. 14, no. 1, pp. 79-88, 2018, doi: 10.1109/TII.2017.2730440.

[16] C. Peng, P. Xie, L. Pan, and R. Yu, "Flexible Robust Optimization Dispatch for Hybrid Wind/Photovoltaic/Hydro/Thermal Power System," *IEEE Transactions on Smart Grid,* vol. 7, no. 2, pp. 751-762, 2016, doi: 10.1109/TSG.2015.2471102.

[17] G. Liu, Y. Xu, and K. Tomsovic, "Bidding Strategy for Microgrid in Day-Ahead Market Based on Hybrid Stochastic/Robust Optimization," *IEEE Transactions on Smart Grid,* vol. 7, no. 1, pp. 227-237, 2016, doi: 10.1109/TSG.2015.2476669.

[18] C. Lee, C. Liu, S. Mehrotra, and Z. Bie, "Robust Distribution Network Reconfiguration," *IEEE Transactions on Smart Grid,* vol. 6, no. 2, pp. 836-842, 2015, doi: 10.1109/TSG.2014.2375160.

[19] T. Zhao, X. Pan, S. Yao, C. Ju, and L. Li, "Strategic Bidding of Hybrid AC/DC Microgrid Embedded Energy Hubs: A Two-Stage Chance Constrained Stochastic Programming Approach," *IEEE Transactions on Sustainable Energy,* vol. 11, no. 1, pp. 116-125, 2020, doi: 10.1109/TSTE.2018.2884997.

[20] A. Najafi, H. Falaghi, J. Contreras, and M. Ramezani, "A Stochastic Bilevel Model for the Energy Hub Manager Problem," *IEEE Transactions on Smart Grid,* vol. 8, no. 5, pp. 2394-2404, 2017, doi: 10.1109/TSG.2016.2618845.

[21] R. Hemmati, "Stochastic energy investment in off-grid renewable energy hub for autonomous building," *IET Renewable Power Generation,* vol. 13, no. 12, pp. 2232-2239, 2019, doi: 10.1049/iet-rpg.2018.6254.

[22] X. Lu, K. W. Chan, S. Xia, B. Zhou, and X. Luo, "Security-Constrained Multiperiod Economic Dispatch With Renewable Energy Utilizing Distributionally Robust Optimization," *IEEE Transactions on Sustainable Energy,* vol. 10, no. 2, pp. 768-779, 2019, doi: 10.1109/TSTE.2018.2847419.

[23] X. Lu, K. W. Chan, S. Xia, X. Zhang, G. Wang, and F. Li, "A Model to Mitigate Forecast Uncertainties in Distribution Systems Using the Temporal Flexibility of EVAs," *IEEE Transactions on Power Systems,* vol. 35, no. 3, pp. 2212-2221, 2020, doi: 10.1109/TPWRS.2019.2951108.

[24] S. Li, H. He, C. Su, and P. Zhao, "Data driven battery modeling and management method with aging phenomenon considered," *Applied Energy,* vol. 275, p. 115340, 2020/10/01/ 2020, doi: https://doi.org/10.1016/j.apenergy.2020.115340.

[25] E. Delage and Y. Ye, "Distributionally robust optimization under moment uncertainty with application to data-driven problems," *Operations research,* vol. 58, no. 3, pp. 595-612, 2010.

[26] Y. Chen, W. Wei, F. Liu, and S. Mei, "Distributionally robust hydro-thermal-wind economic dispatch," *Applied Energy,* vol. 173, pp. 511-519, 2016/07/01/ 2016, doi: https://doi.org/10.1016/j.apenergy.2016.04.060.

[27] W. Ben-Ameur and J. Neto, "A constraint generation algorithm for large scale linear programs using multiple-points separation," *Mathematical Programming,* vol. 107, no. 3, pp. 517-537, 2006/07/01 2006, doi: 10.1007/s10107-005-0694-0.